Conditional Synthesis of 3D Molecules with Time Correction Sampler

Hojung Jung^{1*} Youngrok Park^{1*} Laura Schmid¹ Jaehyeong Jo¹ Dongkyu Lee² Bongsang Kim² Se-Young Yun^{1†} Jinwoo Shin^{1†} KAIST AI¹ LG Electronics² {ghwjd7281, yr-park, yunseyoung, jinwooshin}@kaist.ac.kr

Abstract

Diffusion models have demonstrated remarkable success in various domains, including molecular generation. However, conditional molecular generation remains a fundamental challenge due to an intrinsic trade-off between targeting specific chemical properties and generating meaningful samples from the data distribution. In this work, we present Time-Aware Conditional Synthesis (TACS), a novel approach to conditional generation on diffusion models. It integrates adaptively controlled plug-and-play "online" guidance into a diffusion model, driving samples toward the desired properties while maintaining validity and stability. A key component of our algorithm is our new type of diffusion sampler, Time Correction Sampler (TCS), which is used to control guidance and ensure that the generated molecules remain on the correct manifold at each reverse step of the diffusion process at the same time. Our proposed method demonstrates significant performance in conditional 3D molecular generation and offers a promising approach towards inverse molecular design, potentially facilitating advancements in drug discovery, materials science, and other related fields.

1 Introduction

Discovering molecules with specific target properties is a fundamental challenge in modern chemistry, with significant implications for various domains such as drug discovery and materials science [49, 44, 7]. While diffusion models have shown great success in the generation of real-world molecules [55, 31], their primary goal is often simply to generate realistic molecules without considering specific properties, which can lead to producing molecules with undesirable chemical properties.

Existing works address this issue by leveraging controllable diffusion frameworks to generate molecules with desired properties [23, 5]. One approach is to use classifier guidance [54], which utilizes auxiliary trained classifiers to guide the diffusion process [5]. An alternative is to use classifier-free guidance (CFG) [19], which directly trains the diffusion models on condition-labeled data. While both approaches can generate stable molecules, they struggle to generate truly desirable molecules due to the complex structures and the discrete nature of atomic features [24].

On the other hand, recent works [51, 18] have introduced training-free guidance for controllable generation in a plug-and-play manner, which we hereafter refer to as online guidance (OG). This approach can directly estimate the conditional score with unconditional diffusion model. However, our analysis shows that applying online guidance into the molecular generation can result in generating samples with significantly low molecular stability and validity due to the stepwise enforcement of specific conditions without considering the original distribution at each timestep.

75914

38th Conference on Neural Information Processing Systems (NeurIPS 2024).

^{*}Equal contribution

[†]Corresponding authors

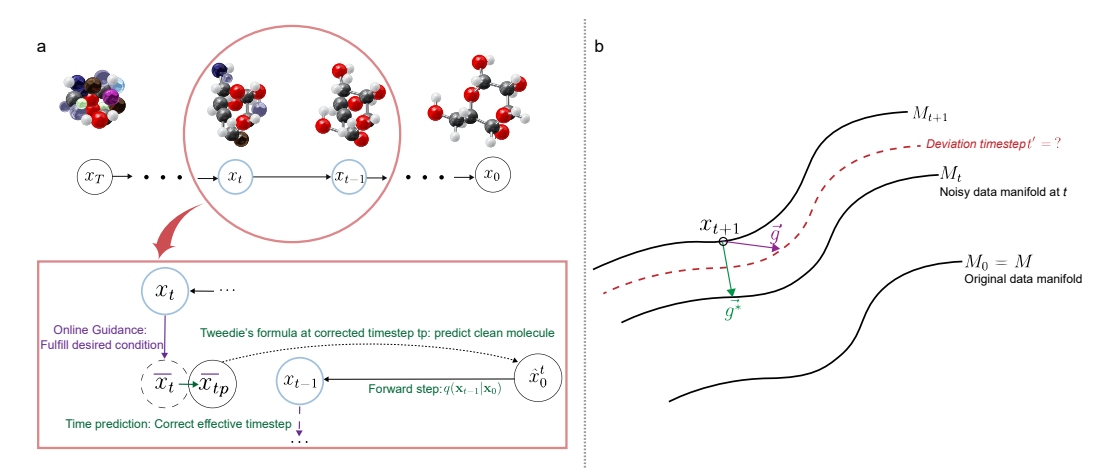


Figure 1: (a) Overview of Time-Aware Conditional Synthesis (TACS). TACS helps generate high-quality samples that match target condition while following basic properties of the molecules. At each timestep t, online guidance is applied to push x_t towards the desired condition. Time Predictor finds the desired timestep t_p for x_t after applying the guidance. Using predicted timestep t_p , Tweedie's formula is used to predict the clean molecule \hat{x}_0^t . Finally, forward process $q(x_{t-1}|x_0)$ is applied to proceed to the next denoising step of t-1. (b) Motivation for TACS. Applying online guidance (\vec{g} , purple) can shift the generated samples away from the correct data manifold corresponding to the current timestep. This undesirable deviation (red) can be avoided by using time correction to first measure the deviated timestep t', then adjusting the guidance to get corrected guidance vector ($\vec{g*}$, green), which keeps the generated samples stay on the correct data manifold.

To address this gap, we propose *Time-Aware Conditional Synthesis* (TACS), a novel framework for generating 3D molecules. TACS utilizes the online guidance in tandem with a novel diffusion sampling technique that we call *Time Correction Sampler* (TCS). TCS explicitly considers the possibility that online guidance can steer the generated sample away from the desired data manifold at each step of the diffusion model's denoising process, resulting in an 'effective timestep' that does not match the correct timestep during the generation. TCS then corrects this mismatch between the timesteps, thereby effectively preventing samples from deviating from the target distribution while ensuring they satisfy the desired conditions. By combining online guidance with TCS and integrating them into a diffusion model, TACS allows generated samples to strike a balance between approaching the target property and remaining faithful to the target distribution throughout the denoising process.

To the best of our knowledge, TACS is the first diffusion framework that simultaneously addresses inverse molecular design and data consistency, two critical objectives that often conflict.

We summarize our main contributions as follows:

- We propose Time-Aware Conditional Synthesis (TACS), a new framework for diffusion model that utilizes adaptively corrected online guidance during the generation.
- We introduce Time Correction Sampler (TCS), a novel diffusion sampling technique that ensures
 the generated samples remain faithful to the data distribution. It includes a time predictor, an
 equivariant graph neural network that accurately estimates the correct data manifold during
 inference by predicting the time information of the generation process.
- Through extensive experiments on a 3D molecule dataset, we demonstrate that TACS outperforms previous state-of-the-art methods by producing samples that closely match the desired quantum chemical properties while maintaining data consistency.

2 Related Works

Diffusion models Diffusion models have achieved great success in a variety of domains, including generation of images [12, 46], audio generation [30], videos [21, 36, 42], and point clouds [8, 37]. A particular highlight in the success of diffusion models is their potential to generate molecules that

can form the basis of new, previously unseen, medical compounds. Multiple approaches have been explored to achieve this. For instance, graph diffusion such as GeoDiff [57], GDSS [26], and Di-Gress [54] can generate graph structures that correspond to molecular candidates. Additionally, some approaches incorporate chemical knowledge tailored to specific applications, such as RFdiffusion for protein design [55], a method based on the RoseTTAFold structure prediction network [31]. Other previous literature considers different domain-specific applications, such as diffusion for molecular docking [11], or molecular conformer generation [25]. Most relevant to our work, diffusion models have also shown promising results in synthesizing 3D molecules [23, 58, 27], generating stable and valid 3D structures. Recently, some of the works further advance 3D molecule generation techniques by making more reliable diffusion process [63] or fast generation [22] of 3D molecules.

Conditional molecular generation Deep generative models [38, 23, 58] have made considerable progress in synthesizing 3D molecules with specific properties. Specifically, conditional diffusion models [23, 5, 58, 18] have achieved noticeable improvements in synthesizing realistic molecules. EDM [23] trains separate conditional diffusion models for each type of chemical condition, while EEGSDE [5] trains an additional energy-based model to provide conditional guidance during the inference. GeoLDM [58] utilizes a latent diffusion model [46] to run the diffusion process in the latent space. MuDM [18] applies online guidance to simultaneously target multiple properties. However, existing methods either produce unstable and invalid molecular structures or are unable to accurately meet the target conditions. To overcome these limitations, we propose TACS, a novel framework which ensures the generative process remains faithful to the learned marginal distributions in each timestep while effectively guiding the samples to meet the desired quantum chemical properties.

Adaptive inference schedule Recent efforts have explored adaptive inference schedules to enhance the fidelity of samples generated by diffusion models with timestep information. [59] proposes adjusting the noise schedule during reverse diffusion, while [60] optimizes input timesteps for a more accurate reverse trajectory. TS-DPM [34] mitigates exposure bias by adaptively shifting timesteps during inference to align with the training variance. Similar to our time preidction mechanism, several works leverage auxilary network to classify time information with different motivation and purpose. DMCMC [28] introduce noise classifier for accelerating inference during earlier diffusion steps and MoreRed [61] leverages a timestep prediction network to initialize or adaptively guide the reverse diffusion process using the adjusted timesteps for molecular relaxation. In contrast, our TACS is specifically designed for conditional generation, predicts timesteps at each denoising step to refine clean sample estimates via Tweedie's formula, ensuring alignment with the data manifold and adherence to target conditions. Further comparison is provided in Appendix E.

3 Preliminaries

Diffusion models Diffusion models [50, 20, 52] are a type of generative model that learn to reverse a multi-step forward noising process applied to the given data. In the forward process, noise is gradually injected into the ground truth data, $\mathbf{x_0} \sim q_0$, until it becomes perturbed into random noise, $\mathbf{x}_T \sim \mathcal{N}(0, \mathbf{I})$, where T is the total number of diffusion steps. We follow the Variance Preserving stochastic differential equation (VP-SDE) [52, 20] where the forward process is modeled by the following SDE:

$$d\mathbf{x}_t = -\frac{1}{2}\beta(t)\mathbf{x}_t dt + \sqrt{\beta(t)}d\mathbf{w}_t, \tag{1}$$

where $\beta(t)$ is a pre-defined noise schedule and \mathbf{w}_t is a standard Wiener process. Then, the reverse of the forward process in Eq. (1) is also a diffusion process that is modeled by the following SDE [2]:

$$d\mathbf{x}_{t} = \left[-\frac{1}{2}\beta(t)\mathbf{x}_{t} - \beta(t)\nabla_{\mathbf{x}_{t}}\log p_{t}(\mathbf{x}_{t}) \right] dt + \sqrt{\beta(t)}d\mathbf{\bar{w}}_{t},$$
 (2)

where p_t is the probability density of \mathbf{x}_t and $\bar{\mathbf{w}}_t$ is a standard Wiener process with backward time flows. The reverse process in Eq. (2) can be used as a generative model when the score function $\nabla_{\mathbf{x}} \log p_t(\mathbf{x})$ is known. To estimate the score function from given data, a neural network s_{θ} is trained to minimize the following objective [52]:

$$\mathcal{L}(\boldsymbol{\theta}) = \mathbb{E}_{t,\mathbf{x}_0} \lambda(t) \| \boldsymbol{s}_{\boldsymbol{\theta}}(\mathbf{x}_t, t) - \nabla_{\mathbf{x}_t} \log p_t(\mathbf{x}_t) \|_2^2, \tag{3}$$

where $t \sim U[0,T]$, \mathbf{x}_0 is sampled from the data distribution, and $\lambda : [0,T] \to \mathbb{R}^+$ is a positive weight function.

Online guidance Recent works [17, 9, 51] leverage a conditional diffusion process where the conditional probability $p_t(\mathbf{x}_t|\mathbf{c})$ is modeled without training on labeled pairs $(\mathbf{x}_t,\mathbf{c})$. To understand this approach, observe that for the conditional generation, the reverse SDE of Eq. (2) can be rewritten as follows:

$$d\mathbf{x}_{t} = \left[-\frac{1}{2}\beta(t)\mathbf{x}_{t} - \beta(t)\nabla_{\mathbf{x}_{t}}\log p_{t}(\mathbf{x}_{t}|\mathbf{c}) \right] dt + \sqrt{\beta(t)}d\bar{\mathbf{w}}_{t}.$$
 (4)

From Bayes' rule, the conditional score $\nabla_{\mathbf{x}} \log p_t(\mathbf{x}_t | \mathbf{c})$ can be decomposed as follows:

$$\nabla_{\mathbf{x}_t} \log p_t(\mathbf{x}_t | \mathbf{c}) = \nabla_{\mathbf{x}_t} \log p_t(\mathbf{x}_t) + \nabla_{\mathbf{x}_t} \log p_t(\mathbf{c} | \mathbf{x}_t). \tag{5}$$

While unconditional score $\nabla_{\mathbf{x}_t} \log p_t(\mathbf{x}_t)$ can be approximated by the unconditional diffusion model s_{θ} from Eq. (3), online guidance can estimate conditional score part $\nabla_{\mathbf{x}_t} \log p(\mathbf{c}|\mathbf{x}_t)$ without any training. Notably, DPS [9] approximates conditional score as follows:

$$\nabla_{\mathbf{x}_t} \log p(\mathbf{c}|\mathbf{x}_t) \approx \nabla_{\mathbf{x}_t} \log p(\mathbf{c}|\hat{\mathbf{x}}_0), \tag{6}$$

where $\hat{\mathbf{x}}_0$ is a point estimation of the final clean data using Tweedie's formula [13]:

$$\hat{\mathbf{x}}_0 = \frac{\mathbf{x}_t + (1 - \bar{\alpha}_t) \nabla_{\mathbf{x}_t} \log p(\mathbf{x}_t)}{\sqrt{\bar{\alpha}_t}}, \ \bar{\alpha}_t = e^{-\frac{1}{2} \int_0^t \beta(s) ds}.$$
 (7)

While DPS uses a point estimate of \mathbf{x}_0 , Loss Guided Diffusion (LGD) [51] uses Bayesian assumption where \mathbf{x}_0 is a Monte Carlo estimation of $q(\mathbf{x}_0|\mathbf{x}_t)$, which is a normal distribution with mean $\hat{\mathbf{x}}_0$ and variance σ_t^2 which is a hyperparameter.

For a given property estimator A satisfying $\mathbf{c} = A(\mathbf{x}_0)$, Eq. (6) can be written as follows:

$$\nabla_{\mathbf{x}_t} \log \mathbb{E}_{\mathbf{x}_0 \sim p(\mathbf{x}_0 | \mathbf{x}_t)} p(\mathbf{c} | \hat{\mathbf{x}}_0) \approx \nabla_{\mathbf{x}_t} \log \left(\frac{1}{m} \sum_{i=1}^m \exp\left(-\mathcal{L}(\mathcal{A}(\mathbf{x}_0^i), \mathbf{c}) \right) \right) =: \mathbf{g}(\mathbf{x}_t, t), \quad (8)$$

where \mathcal{L} is a differentiable loss function and \mathbf{x}_0^i are independent variables sampled from $q(\mathbf{x}_0|\mathbf{x}_t)$. Using this approximation, we can replace $\nabla_{\mathbf{x}_t} \log p(\mathbf{c}|\mathbf{x}_t)$ in Eq. (5) and conditional generation process now becomes:

$$d\mathbf{x}_{t} = \left[-\frac{1}{2}\beta(t)\mathbf{x}_{t} - \beta(t) \left(\nabla_{\mathbf{x}_{t}} \log p_{t}(\mathbf{x}_{t}) + z\mathbf{g}(\mathbf{x}_{t}, t) \right) \right] dt + \sqrt{\beta(t)} d\mathbf{\bar{w}}_{t},$$
(9)

where z is the hyperparameter for controlling online guidance strength. In this work, we use L_2 loss for the differentiable loss \mathcal{L} and set m=1 following Song et al. [51].

3D representations of molecules In our framework, we follow EDM [23] in modeling the distribution of atomic coordinates x within a linear subspace \mathcal{X} , where the center of mass is constrained to zero. This allows for translation-invariant modeling of molecular geometries. Further details of the zero-center-of-mass subspace is provided in Appendix A.3.

4 Time-Aware Conditional Synthesis

In this section, we propose our framework, Time-Aware Conditional Synthesis (TACS). Section 4.1 presents the key component of TACS: the Time Correction Sampler, a novel sampling technique that leverages corrected time information during the generation process. Section 4.2 introduces the overall framework of TACS, which accurately integrates online guidance into the diffusion process using our sampling technique to generate stable and valid molecules that meet the target conditions.

4.1 Time Correction Sampler

Diffusion models are known to have an inherent bias, referred to as exposure bias, where the marginal distributions of the forward process do not match the learned marginal distributions of the backward process [40]. To mitigate exposure bias in the diffusion models, we propose the Time Correction Sampler (TCS), which consists of two parts: time prediction and time correction.

Algorithm 1 Time-Aware Conditional Synthesis (TACS)

Input: Total number of diffusion timesteps T, online guidance strength z, target condition c, diffusion model θ , time predictor ϕ , time-clip window size Δ .

```
1: \mathbf{x}_T \sim \mathcal{N}(0, \mathbf{I}_d)
 2: for t = T to 1 do
            if Online guidance then
                  \mathbf{g}(\mathbf{x}_t, t) = -\nabla_{\mathbf{x}_t} \mathcal{L}(\mathcal{A}(\mathbf{x}_0), \mathbf{c})
                                                                                                                                       > Online guidance from Eq. (8)
                 \mathbf{x}_t' \leftarrow \mathbf{x}_t + z \cdot \mathbf{g}(\mathbf{x}_t, t)
                 t_{\text{pred}} \leftarrow \arg\max\left(\phi(\mathbf{x}_t')\right)
 6:
                 t_{\text{pred}} \leftarrow \text{clip}(t_{\text{pred}}, \Delta)
                 \hat{\mathbf{x}}_0' \leftarrow \mathsf{Tweedie}(\mathbf{x}_t', t_{\mathsf{pred}})
 8:
                                                                                                                                                                       \triangleright from Eq. (11)
 9:
                 \mathbf{x}_{t-1} \leftarrow \mathtt{forward}(\hat{\mathbf{x}}_0', t-1)
                                                                                                                                                                           \triangleright from Eq. (1)
10:
                 \mathbf{x}_{t-1} \leftarrow \mathtt{reverse}(\mathbf{x}_t, t)
                                                                                                                           ⊳ one reverse step by diffusion model
11:
             end if
12:
13: end for
```

Time Predictor During conditional generation process of diffusion model, a sample follows the reverse SDE as in Eq. (4). However, due to error accumulation during the generation process [33, 6], a sample at timestep t of the reverse process of diffusion may not accurately reflect the true marginal distribution at timestep t. This discrepancy between forward and reverse process can especially increased when applying online guidance for every denoising steps and consequently lead to the generation of molecules with low stability and validity. We aim to mitigate this issue by correcting the time information based on the sample's current position.

To achieve this, we train a neural network, a time predictor, to estimate the proper timestep of a given noised data. Specifically, given a random data point ${\bf x}$ with unknown timestep, time predictor models how likely ${\bf x} \sim p_t$ for each timestep in [0,T]. For training, we parameterize a time predictor by equivariant graph neural network (EGNN) ϕ . Then, cross-entropy loss between the one hot embedding of timestep vector and the logit vector for the model output is used as follows:

$$\mathcal{L}_{tp}(\boldsymbol{\phi}) = -\mathbb{E}_{t,\mathbf{x}_0} \left[\log \left(\hat{\mathbf{p}}_{\boldsymbol{\phi}}(\mathbf{x}_t)_t \right) \right], \tag{10}$$

where timestep t is sampled from the uniform distribution U[0,T], \mathbf{x}_0 is chosen from the data distribution, \mathbf{x}_t is constructed from Eq. (1), and $\hat{\mathbf{p}}_{\phi}(\mathbf{x}_t)_t$ is the t-th component of the model output $\hat{\mathbf{p}}_{\phi}$ for a given input \mathbf{x}_t . We empirically evaluate the performance of the time predictor on the QM9 train and test datasets. Forward noise, corresponding to each true timestep, is added to the data, and the time predictor estimates the true timestep, with accuracy measured accordingly. As shown in 3b, the predictor struggles in the white noise region, but achieves near-perfect accuracy after timestep 400.

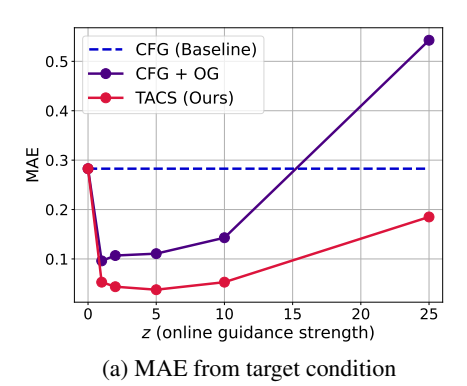
Time correction TCS works by first modifying Tweedie's formula (Eq. 7) using the estimated timestep from time predictor to utilize the information of the proper timestep estimated by time predictor during the denoising diffusion process.

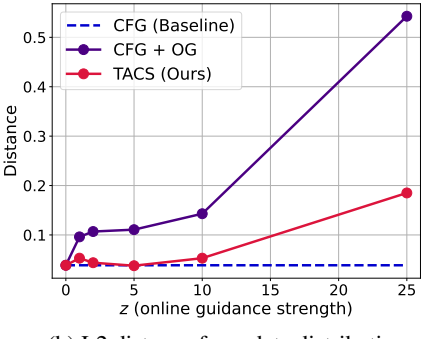
Specifically, for a sample $\tilde{\mathbf{x}}_t$ at time t during the reverse diffusion process, we use the corrected timestep t_{pred} predicted by time predictor, instead of the current timestep t, to estimate the final sample $\hat{\mathbf{x}}_0$ as follows:

$$\mathsf{Tweedie}(\tilde{\mathbf{x}}_t, t_{\mathsf{pred}}) := f(\tilde{\mathbf{x}}_t, t_{\mathsf{pred}}) = \frac{\tilde{\mathbf{x}}_t + (1 - \bar{\alpha}_{t_{\mathsf{pred}}}) s_{\boldsymbol{\theta}}(\tilde{\mathbf{x}}_t, t_{\mathsf{pred}})}{\sqrt{\bar{\alpha}_{t_{\mathsf{pred}}}}}. \tag{11}$$

From the better prediction of the final sample $\hat{\mathbf{x}}_0$, we perturb it back to the next timestep t-1 using the forward process using Eq. (1).

Intuitively, TCS encourages the generated samples to adhere more closely to the proper data manifolds at each denoising step. The iterative correction of the time through the generative process ensures the final sample lie on the correct data distribution. Consequently, for 3D molecular generation, TCS helps synthesizing molecules with higher molecular stability and validity, both of which are crucial for generating realistic and useful molecules.





(b) L2 distance from data distribution

Figure 2: Synthetic experiment on H_3^+ dataset. TACS is robust in generating samples that (a) match the desired condition and (b) stick to the original data distribution.

4.2 Unified guidance with time correction

Finally, we present TACS in Algorithm 1, which is a novel diffusion sampler for conditional generation that integrates TCS with online guidance. For each timestep of the reverse diffusion process (Eq. 4), we apply online guidance (Eq. 8) to guide the process toward satisfying the target condition. Subsequently, TCS is applied to correct the deviation from the proper marginal distribution induced by online guidance. This ensures the samples follow the correct marginal distribution during the generative process, as shown in Fig. 1. In Section 5, we experimentally validate that TACS is capable of generating valid and stable molecules satisfying the target condition.

Time clipping During the generation, we empirically observe that the predicted timestep $t_{\rm pred}$ often deviates significantly from the current time step t. Naively applying this information to TCS can be problematic as the dramatic changes in timestep may skip crucial steps, resulting in unstable or invalid molecules. To prevent large deviation of $t_{\rm pred}$, we set a time window so that $t_{\rm pred}$ remains in the time interval $[t-\Delta,t+\Delta]$, where Δ is a hyperparameter for the window size.

5 Experiments

In this section, we present comprehensive experiments to evaluate the performance of TACS and demonstrate its effectiveness in generating 3D molecular structures with specific properties while maintaining stability and validity. In Section 5.1, we present synthetic experiment with H_3^+ molecules, where the ground state energies are computed using the variational quantum eigensolver (VQE). In Section 5.2, we assess our method using QM9, a standard dataset in quantum chemistry that includes molecular properties and atom coordinates. We compare our approach against several state-of-the-art baselines and provide a detailed analysis of the results.

5.1 Synthetic experiment with H_3^+

Quantum online guidance We present quantum online guidance as a modified version of online guidance where quantum machine learning algorithm for the property estimation of generating molecules. Specifically, we use VQE [53] when calculating the ground state energy of generated molecules. Contrary to prior works [23, 5], which train auxiliary classifiers to estimate each condition, this quantum computational chemistry-based approach can leverage exact calculation of the condition for a given estimate. This, in turn, is expected to generate molecules with accurate target ground state energies. A detailed explanation of this approach is provided in Appendix A.2.

Setup We first construct synthetic H_3^+ as follows. For each molecule, a hydrogen atom is placed uniformly at random within the 3-D unit sphere. We then augment our sample by rotating each molecule randomly to satisfy the equivariance property [23]. Then the ground state energy of each molecule is measured with VQE in order to provide conditional labels. Finally, we train unconditional

Table 1: Conditional generation with target quantum properties on QM9. TACS generate samples with lowest MAE while maintaining similar level of stability and validity as other baselines. TCS can generate molecules with high stability and validity. * notation is marked for the values for the best MAE within methods with molecule stability above 80%.

		$C_v\left(\frac{\operatorname{cal}}{\operatorname{mol} K}\right)$			μ (D)			α (Bohr ³)	
Method	MAE	MS (%)	Valid (%)	MAE	MS (%)	Valid (%)	MAE	MS (%)	Valid (%)
U-bound	6.879 ± 0.015	-	-	1.613±0.003	-	-	8.98±0.020	-	-
EDM	1.072 ± 0.005	81.0 ± 0.6	90.4 ± 0.2	1.118 ± 0.006	80.8 ± 0.2	91.2 ± 0.3	2.77 ± 0.050	79.6 ± 0.3	89.9 ± 0.2
EEGSDE	1.044 ± 0.023	81.0 ± 0.5	90.5 ± 0.2	0.854 ± 0.002	79.4 ± 0.1	90.6 ± 0.5	2.62 ± 0.090	79.8 ± 0.3	89.2 ± 0.3
OG	0.184 ± 0.004	30.2 ± 0.4	51.9 ± 6.8	26.654 ± 8.878	6.8 ± 0.5	29.7 ± 0.3	0.55 ± 0.019	21.2 ± 0.2	48.7 ± 0.3
TCS(ours)	0.904 ± 0.011	90.3 \pm 0.5	94.9 ± 0.1	0.971 ± 0.005	92.7 \pm 0.3	96.6 \pm 0.2	1.85 ± 0.006	87.5 ± 0.2	93.8 ± 0.1
TACS(ours)	$0.659*\pm0.008$	83.6 ± 0.2	92.4 ± 0.1	$0.387^* \pm 0.006$	83.3±0.3	91.3 ± 0.3	1.44*±0.007	86.0 ± 0.1	92.5 ± 0.1
L-bound	0.040	-	-	0.043	-	-	0.090	-	-
		$\Delta\epsilon$ (meV)		($\epsilon_{\mathrm{HOMO}}~(\mathrm{meV})$			ELUMO (meV)	
Method	MAE	MS (%)	Valid (%)	MAE	MS (%)	Valid (%)	MAE	MS (%)	Valid (%)
U-bound	1464±4	-	-	645±41	-	-	1457±5	-	-
EDM	673±7	81.8 ± 0.5	90.9 ± 0.3	372 ± 1	79.6 ± 0.1	91.6 ± 0.2	602 ± 4	81.0 ± 0.2	91.4 ± 0.5
EEGSDE	539±5	80.1 ± 0.4	90.5 ± 0.3	300 ± 5	78.7 ± 0.7	91.2 ± 0.2	494 ± 9	81.4 ± 0.6	91.1 ± 0.2
OG	95.2 ± 4	31.3 ± 0.7	61.9 ± 3.4	233 ± 8	11.5 ± 0.4	40.8 ± 2.6	170±1	21.1 ± 0.5	42.3 ± 0.9
TCS(ours)	594±4	91.9 ±0.4	96.0±0.2	338±5	92.7 ±0.2	96.6±0.2	493±9	91.7 ±3.9	96.2±0.4
TACS(ours)	332 *±3	88.8 ± 0.6	93.9 ± 0.3	$168*\pm 2$	87.3±0.7	93.0 ± 0.2	289 *±4	82.7±0.7	91.3±0.2
L-bound	65	-	-	39	-	-	36	-	-

diffusion model and CFG-based conditional diffusion model with the constructed data. For evaluation, we measure the ground state energy and calculate MAE (Mean Absolute Error) with the target energy. Also, we measure the average L2 distance between position of each atom and its projection to the unit sphere.

Results The results in Figure 2 indicate that while online guidance correctly guides the samples to the target condition, it can lead to the samples deviated from the original data distribution. In contrast, molecules sampled from TACS can satisfy both low MAE and low L2 distance. Further details and additional discussions are provided in Appendix B.1.

5.2 Conditional generation for target quantum chemical properties

Dataset We evaluate our method on QM9 dataset [45], which contains about 134k molecules with up to 9 heavy atoms of (C, N, O, F), each labeled with 12 quantum chemical properties. Following previous works [1, 23], we test on 6 types of quantum chemical properties and split the dataset into 100k/18k/13k molecules for training, validation, and test. The training set is further divided into two disjoint subsets of 50k molecules each: D_a for property predictor training and D_b for generative model training. Further details are provided in Appendix B.2.

Evaluation To evaluate how generate samples meet the desired target condition, a property prediction model ϕ_p [47] is trained on D_a . Then, MAE for K number of samples is calculated as $\frac{1}{K}\sum_{i=1}^K |\phi_p(\mathbf{x}^{(i)}) - c^{(i)}|$, where $\mathbf{x}^{(i)}$ represents i-th generated molecule and $c^{(i)}$ is corresponding target quantum chemical properties. Molecular stability (MS) and validity (Valid) [23] are used to measure how generated samples satisfy basic chemical properties. Details of the evaluation metrics are provided in Appendix B.2.

Baselines We use Equivariant Diffusion Models (EDM) [23] and Equivariant Energy Guided SDE (EEGSDE) [5] for the baselines. Following [23], we put additional baselines including "Naive Upper-Bound" (randomly shuffled property labels), "#Atoms" (properties predicted by atom count), and "L-Bound" (lower bound on MAE using a separate prediction model).

Results Table 1 shows the result of conditional generation of TACS and TCS with baselines. We generate $K=10^4$ samples for the evaluation in each experiment and the average values and standard deviations are reported across 5 runs. For all of the quantum chemical properties, TACS achieves lower MAE while maintaining comparable or higher molecular stability (MS) and validity compared to other baselines. Notably, when comparing with the baseline methods that maintains the MS above 80%, the MAE of TACS is significantly lower than the baselines. The result demonstrates the

75920

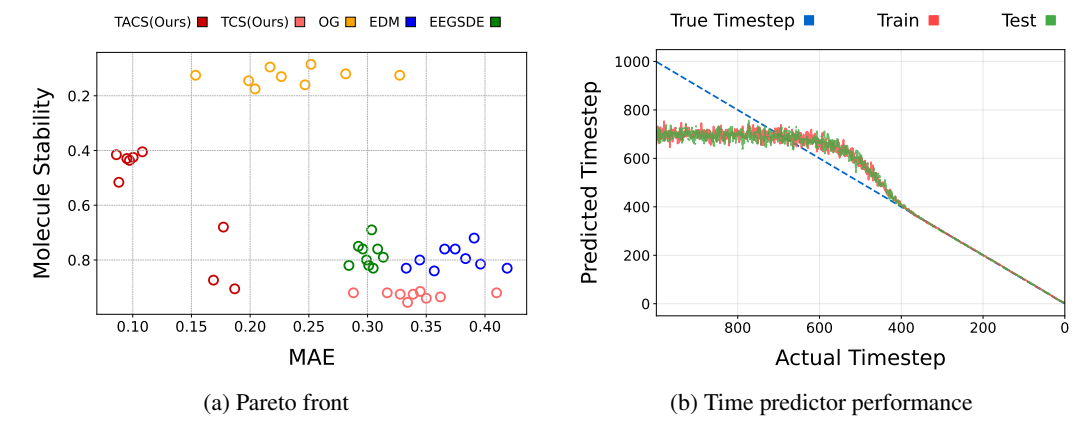


Figure 3: (a) Comparative analysis of molecule stability and MAE across five distinct methods, highlighting the enhanced stability of our approach at comparable MAE levels. (b) Performance of the time predictor for train and test set on QM9.

Table 2: Quantitative results showing similarity and stability of generated molecules compared to target structures.

	QM9			
Method	Similarity ↑	MS (%)		
cG-SchNet	0.499±0.002	-		
Conditional EDM	0.671 ± 0.004	-		
TCS (Ours)	0.792 ± 0.077	90.42		
TACS (Ours) ($z = 0.01$)	0.694 ± 0.001	90.45		
TACS (Ours) ($z = 0.05$)	0.695 ± 0.003	90.02		
TACS (Ours) ($z = 0.1$)	0.713 ± 0.087	90.28		
EEGSDE $(s = 0.1)$	0.547 ± 0.002	74.07		
EEGSDE $(s = 0.5)$	0.600 ± 0.002	74.67		
EEGSDE ($s = 1.0$)	0.540 ± 0.029	90.44		

Table 3: Unconditional generation using Geom-Drug dataset.

	Geom	-Drug
Method	AS (%) ↑	Valid (%)
Data	86.5	99.9
ENF	_	-
G-Schnet	_	-
GDM	75.0	90.8
GDM-AUG	77.7	91.8
EDM	81.3	92.6
EDM-Bridge	82.4	92.8
TCS(Ours)	89.6	97.6

effectiveness of TACS in balancing the objectives of generating molecules with desired properties and ensuring their structural validity.

TCS achieves high validity and atom stability and molecular stability, surpassing the unconditional generation performance of the baselines, but with a higher MAE compared to TACS. This highlights the importance of online guidance for precise property targeting. However, applying only online guidance yields samples with low MAE but suffers from reduced validity and stability, occasionally failing to generate valid molecules due to numerical instability. This shows the ability of TACS which places the samples on the correct data manifold at each denoising step, even if they deviate from the true time-manifold due to the online guidance. Finally, we put the results of different methods with 9 different runs for each method and plot the MAE and MS in Figure 3a. The result clearly shows that TACS and TCS reaches closer to the Pareto front of satisfying molecular stability and the target condition together.

5.3 Target structure generation

We conduct experiments on target structure generation with QM9 as in [5]. For evaluation, we report Tanimoto similarity score [16] which captures similarity of molecular structures by molecular fingerprint and molecular stability to check whether basic properties of molecules are satisfied during the conditional generation process. We put additional details of the experiment in Appendix B.3.2.

Results Table 2 shows that TACS significantly outperforms baseline methods both in Tanimoto similarity and molecular stability. Interestingly, performance of TACS is robust in the online guidance strength z. This demonstrates TACS's ability to generalize on different tasks.

Table 4: Comparison between performance of TACS when using argmax function and expectation for correcting timesteps using time predictor.

	C_v	$\left(\frac{\text{cal}}{\text{mol } K}\right)$	μ	(D)	α (I	Bohr ³)	$\Delta \epsilon$	(meV)	$\epsilon_{ ext{HOM}0}$	(meV)	$\epsilon_{ m LUMO}$	(meV)
Method	MAE	MS (%)	MAE	MS (%)	MAE	MS (%)	MAE	MS (%)	MAE	MS (%)	MAE	MS (%)
Argmax Expectation	0.659 0.703	83.3 84.6	0.387 0.451	83.3 90.2	1.44 1.56	86.0 87.3	332 351	88.8 90.7	168 182	87.3 89.8	289 334	82.7 90.1

5.4 Unconditional generation on Geom-Drug dataset

To verify the scalability of time correction sampler, we use Geom-Drug [4] as our dataset. Geom-Drug consists of much larger and complicate molecules compared to the QM9. For fair comparisons, we follow [23, 5] to split the dataset for training, validation and test set include 554k, 70k, and 70k samples respectively. We test the performance of TCS on unconditional generation of 3D molecules when using Geom-Drug. For evaluation, we use atom stability (AS) and validity of generated samples. The result in Table 3 shows that samples generated by TCS satisfy the highest atom stability and the validity with high margin compared to the baselines. Details of the experiments are in Appendix B.3.1.

5.5 Ablation Studies

Time prediction function We investigate how the design of time prediction function affects the performance of TACS. Specifically, for line 6 in Alg. 1, rather than using argmax function to obtain corrected timestep $t_{\rm pred}$, we choose to use expectation value by $t_{\rm pred} = \mathbb{E}[\phi(x)]$. Table 4 shows the comparison between two methods in six different types of quantum chemical properties. Expectation based time prediction results in molecules with higher MAE and higher molecular stability.

Online guidance strength z To analyze the effect of online guidance strength z in Eq. (9), we measure MAE, molecular stability, and validity of samples generated by TACS for different z values. Table 5 shows the result with target condition on $\epsilon_{\rm LUMO}$ values. One can observe while trade-off occurs for different z values, performance of TACS is robust in varying z. Interestingly, our experiment shows that there exists an optimal value of z which generates samples with the lowest MAE that is even compara-

Table 5: Ablation study on the OG strength z with target property ϵ_{LUMO} .

Method	MAE	MS (%)	Valid (%)
TCS (z = 0)	493	91.7	96.2
OG	170	21.1	42.3
z = 1.5	311	80.3	90.7
z = 1.0	236	74.9	86.3
z = 0.5	288	82.7	91.3

ble to applying online guidance without time correction (OG). As expected, using z=0 (TCS) generates molecules with the highest MS and validity but with the highest MAE.

Time window length Δ We measure how the performance of TACS varies with time winodw length Δ . Table 6 shows the MAE, molecular stability values for different window sizes when the target property is α . The result shows that the performance of TACS is robust when using moderate window size but decreases when window size becomes larger than certain point. We set $\Delta=10$ for other experiments.

In Appendix C, we provide the results of further ablation studies including the effect of mc sampling and effective diffusion steps for TACS. Overall, the results show that our method is robust in the choice of hyperparameters and generalizable to different datasets and tasks.

Table 6: Results of TACS on target property α when varying the time window size.

Window size (Δ)	MAE	MS (%)
2	1.481	87.25
4	1.460	86.52
6	1.460	85.73
8	1.448	86.84
10	1.441	86.08
12	1.442	85.17
14	1.459	82.76
16	1.530	79.10

6 Discussion

Exploiting quantum chemistry In Section 5.1, we demonstrate that quantum computing-based guidance can serve as an accurate property predictor for the online guidance. Currently, in the absence of a non-noisy quantum computer, scaling up this exact guidance to the QM9 dataset is close to impossible due to compounding noise [43, 10]. However, future fault-tolerant quantum technology is

expected to provide quantum advantage in calculating chemical properties. This can be incorporated into our algorithm when using online guidance and therefore, further improvements of our TACS are on the horizon.

Connection to other fields Recent works point out the exposure bias exists for diffusion models [40], where there is a mismatch between forward and reverse process. Our experiments in 5.2 indicate that Time Correction Sampler can provide a solution to the exposure bias problem during the sampling process in diffusion models. Moreover, since time predictor can gauge this mismatch during inference, one might leverage this information for future works.

Another direction is applying our algorithm to matching [56, 27, 39] frameworks. Contrary to diffusion models, these matching models can start with arbitrary distributions and directly learn vector fields. We expect time predictor to be also effective with these types of algorithms. Investigating the connection between our algorithm and matching models will be an interesting future direction.

7 Conclusion

In this work, we introduce Time-Aware Conditional Synthesis (TACS), a novel approach for conditional 3D molecular generation using diffusion models. Our algorithm leverages a Time Correction Sampler (TCS) in combination with online guidance to ensure that generated samples remain on the correct data manifold during the reverse diffusion process. Our experimental results clearly demonstrate the advantage of our algorithm, as it can generate molecules that are close to the target conditions while also being stable and valid. This can be seen as a significant step towards precise and reliable molecular generation.

Despite multiple advantages, several open questions remain. For example, how can we more efficiently use the Time Correction Sampler, or more generally, whether this method improves performance in other domains such as in image generation. We expect that our work will open various opportunities across different domains, such as quantum chemistry and diffusion models.

Limitation Although we demonstrate the effectiveness of our algorithm on multiple datasets and tasks, we use a trained neural network to estimate chemical properties of each molecule for main experiments. Using exact computational chemistry-based methods might improve our algorithm.

Societal impacts We believe that our framework can assist in drug discovery, which requires synthesizing stable and valid molecules that satisfy target conditions. However, our work could unfortunately be misused to generate toxic or harmful substances.

Acknowledgments

This work was supported by Institute for Information & communications Technology Planning & Evaluation (IITP) grant funded by the Korea government (MSIT) (No. RS-2019-II190075, Artificial Intelligence Graduate School Program (KAIST); No. RS-2024-00457882, AI Research Hub Project), the National Research Foundation of Korea NRF grant funded by the Korean government (MSIT) (No. RS-2019-NR040050 Stochastic Analysis and Application Research Center (SAARC)), and LG Electronics.

References

- [1] Brandon Anderson, Truong Son Hy, and Risi Kondor. Cormorant: Covariant molecular neural networks. *Advances in neural information processing systems*, 32, 2019.
- [2] Brian DO Anderson. Reverse-time diffusion equation models. *Stochastic Processes and their Applications*, 12(3):313–326, 1982.
- [3] Frank Arute, Kunal Arya, Ryan Babbush, Dave Bacon, Joseph C Bardin, Rami Barends, Rupak Biswas, Sergio Boixo, Fernando GSL Brandao, David A Buell, et al. Quantum supremacy using a programmable superconducting processor. *Nature*, 574(7779):505–510, 2019.
- [4] Simon Axelrod and Rafael Gomez-Bombarelli. Geom, energy-annotated molecular conformations for property prediction and molecular generation. *Scientific Data*, 9(1):185, 2022.
- [5] Fan Bao, Min Zhao, Zhongkai Hao, Peiyao Li, Chongxuan Li, and Jun Zhu. Equivariant energy-guided sde for inverse molecular design. In *The eleventh international conference on learning representations*, 2022.
- [6] Joe Benton, VD Bortoli, Arnaud Doucet, and George Deligiannidis. Nearly d-linear convergence bounds for diffusion models via stochastic localization. 2024.
- [7] Keith T Butler, Daniel W Davies, Hugh Cartwright, Olexandr Isayev, and Aron Walsh. Machine learning for molecular and materials science. *Nature*, 559(7715):547–555, 2018.
- [8] Ruojin Cai, Guandao Yang, Hadar Averbuch-Elor, Zekun Hao, Serge J. Belongie, Noah Snavely, and Bharath Hariharan. Learning gradient fields for shape generation. In *ECCV*, 2020.
- [9] Hyungjin Chung, Jeongsol Kim, Michael T Mccann, Marc L Klasky, and Jong Chul Ye. Diffusion posterior sampling for general noisy inverse problems. *arXiv preprint arXiv:2209.14687*, 2022.
- [10] Jacob M. Clary, Eric B. Jones, Derek Vigil-Fowler, Christopher Chang, and Peter Graf. Exploring the scaling limitations of the variational quantum eigensolver with the bond dissociation of hydride diatomic molecules. *International Journal of Quantum Chemistry*, 123(11):e27097, 2023. doi: https://doi.org/10.1002/qua.27097.
- [11] Gabriele Corso, Hannes Stärk, Bowen Jing, Regina Barzilay, and Tommi S. Jaakkola. Diffdock: Diffusion steps, twists, and turns for molecular docking. In *The Eleventh International Conference on Learning Representations*, 2023.
- [12] Prafulla Dhariwal and Alexander Nichol. Diffusion models beat gans on image synthesis. *Advances in neural information processing systems*, 34:8780–8794, 2021.
- [13] Bradley Efron. Tweedie's formula and selection bias. *Journal of the American Statistical Association*, 106(496):1602–1614, 2011.
- [14] Richard P Feynman. Simulating physics with computers. In *Feynman and computation*, pages 133–153. CRC Press, 2018.
- [15] Niklas Gebauer, Michael Gastegger, and Kristof Schütt. Symmetry-adapted generation of 3d point sets for the targeted discovery of molecules. Advances in neural information processing systems, 32, 2019.
- [16] Niklas WA Gebauer, Michael Gastegger, Stefaan SP Hessmann, Klaus-Robert Müller, and Kristof T Schütt. Inverse design of 3d molecular structures with conditional generative neural networks. *Nature communications*, 13(1):973, 2022.
- [17] Alexandros Graikos, Nikolay Malkin, Nebojsa Jojic, and Dimitris Samaras. Diffusion models as plug-and-play priors. Advances in Neural Information Processing Systems, 35:14715–14728, 2022.
- [18] Xu Han, Caihua Shan, Yifei Shen, Can Xu, Han Yang, Xiang Li, and Dongsheng Li. Training-free multi-objective diffusion model for 3d molecule generation. In *The Twelfth International Conference on Learning Representations*, 2023.

- [19] Jonathan Ho and Tim Salimans. Classifier-free diffusion guidance. arXiv preprint arXiv:2207.12598, 2022.
- [20] Jonathan Ho, Ajay Jain, and Pieter Abbeel. Denoising diffusion probabilistic models. Advances in neural information processing systems, 33:6840–6851, 2020.
- [21] Jonathan Ho, Tim Salimans, Alexey Gritsenko, William Chan, Mohammad Norouzi, and David J Fleet. Video diffusion models. *Advances in Neural Information Processing Systems*, 35:8633–8646, 2022.
- [22] Haokai Hong, Wanyu Lin, and Kay Chen Tan. Fast 3d molecule generation via unified geometric optimal transport. *arXiv preprint arXiv:2405.15252*, 2024.
- [23] Emiel Hoogeboom, Victor Garcia Satorras, Clément Vignac, and Max Welling. Equivariant diffusion for molecule generation in 3d. In *International conference on machine learning*, pages 8867–8887. PMLR, 2022.
- [24] Frank Jensen. Introduction to computational chemistry. John wiley & sons, 2017.
- [25] Bowen Jing, Gabriele Corso, Jeffrey Chang, Regina Barzilay, and Tommi Jaakkola. Torsional diffusion for molecular conformer generation. Advances in Neural Information Processing Systems, 35:24240–24253, 2022.
- [26] Jaehyeong Jo, Seul Lee, and Sung Ju Hwang. Score-based generative modeling of graphs via the system of stochastic differential equations. In *International Conference on Machine Learning*, pages 10362–10383. PMLR, 2022.
- [27] Jaehyeong Jo, Dongki Kim, and Sung Ju Hwang. Graph generation with diffusion mixture. *arXiv preprint arXiv:2302.03596*, 2023.
- [28] Beomsu Kim and Jong Chul Ye. Denoising mcmc for accelerating diffusion-based generative models. *arXiv preprint arXiv*:2209.14593, 2022.
- [29] Jonas Köhler, Leon Klein, and Frank Noé. Equivariant flows: exact likelihood generative learning for symmetric densities. In *International conference on machine learning*, pages 5361–5370. PMLR, 2020.
- [30] Zhifeng Kong, Wei Ping, Jiaji Huang, Kexin Zhao, and Bryan Catanzaro. Diffwave: A versatile diffusion model for audio synthesis. *arXiv* preprint arXiv:2009.09761, 2020.
- [31] Rohith Krishna, Jue Wang, Woody Ahern, Pascal Sturmfels, Preetham Venkatesh, Indrek Kalvet, Gyu Rie Lee, Felix S Morey-Burrows, Ivan Anishchenko, Ian R Humphreys, et al. Generalized biomolecular modeling and design with rosettafold all-atom. *Science*, page eadl2528, 2024.
- [32] Greg Landrum et al. Rdkit: Open-source cheminformatics software. 2016.
- [33] Holden Lee, Jianfeng Lu, and Yixin Tan. Convergence for score-based generative modeling with polynomial complexity. Advances in Neural Information Processing Systems, 35:22870–22882, 2022.
- [34] Mingxiao Li, Tingyu Qu, Ruicong Yao, Wei Sun, and Marie-Francine Moens. Alleviating exposure bias in diffusion models through sampling with shifted time steps. *arXiv* preprint *arXiv*:2305.15583, 2023.
- [35] Sijia Liu, Pin-Yu Chen, Bhavya Kailkhura, Gaoyuan Zhang, Alfred O Hero III, and Pramod K Varshney. A primer on zeroth-order optimization in signal processing and machine learning: Principals, recent advances, and applications. *IEEE Signal Processing Magazine*, 37(5):43–54, 2020.
- [36] Yixin Liu, Kai Zhang, Yuan Li, Zhiling Yan, Chujie Gao, Ruoxi Chen, Zhengqing Yuan, Yue Huang, Hanchi Sun, Jianfeng Gao, et al. Sora: A review on background, technology, limitations, and opportunities of large vision models. *arXiv preprint arXiv:2402.17177*, 2024.
- [37] Shitong Luo and Wei Hu. Diffusion probabilistic models for 3d point cloud generation. In *CVPR*, 2021.

- [38] Youzhi Luo and Shuiwang Ji. An autoregressive flow model for 3d molecular geometry generation from scratch. In *International Conference on Learning Representations (ICLR)*, 2022.
- [39] Laurence Midgley, Vincent Stimper, Javier Antorán, Emile Mathieu, Bernhard Schölkopf, and José Miguel Hernández-Lobato. Se (3) equivariant augmented coupling flows. Advances in Neural Information Processing Systems, 36, 2024.
- [40] Mang Ning, Mingxiao Li, Jianlin Su, Albert Ali Salah, and Itir Onal Ertugrul. Elucidating the exposure bias in diffusion models. *arXiv preprint arXiv:2308.15321*, 2023.
- [41] Alberto Peruzzo, Jarrod McClean, Peter Shadbolt, Man-Hong Yung, Xiao-Qi Zhou, Peter J Love, Alán Aspuru-Guzik, and Jeremy L O'brien. A variational eigenvalue solver on a photonic quantum processor. *Nature communications*, 5(1):4213, 2014.
- [42] Adam Polyak, Amit Zohar, Andrew Brown, Andros Tjandra, Animesh Sinha, Ann Lee, Apoorv Vyas, Bowen Shi, Chih-Yao Ma, Ching-Yao Chuang, et al. Movie gen: A cast of media foundation models. *arXiv preprint arXiv:2410.13720*, 2024.
- [43] John Preskill. Quantum computing in the nisq era and beyond. Quantum, 2:79, 2018.
- [44] Edward O Pyzer-Knapp, Changwon Suh, Rafael Gómez-Bombarelli, Jorge Aguilera-Iparraguirre, and Alán Aspuru-Guzik. What is high-throughput virtual screening? a perspective from organic materials discovery. *Annual Review of Materials Research*, 45:195–216, 2015.
- [45] Raghunathan Ramakrishnan, Pavlo O Dral, Matthias Rupp, and O Anatole Von Lilienfeld. Quantum chemistry structures and properties of 134 kilo molecules. *Scientific data*, 1(1):1–7, 2014.
- [46] Robin Rombach, Andreas Blattmann, Dominik Lorenz, Patrick Esser, and Björn Ommer. High-resolution image synthesis with latent diffusion models. In *Proceedings of the IEEE/CVF conference on computer vision and pattern recognition*, pages 10684–10695, 2022.
- [47] Victor Garcia Satorras, Emiel Hoogeboom, and Max Welling. E (n) equivariant graph neural networks. In *International conference on machine learning*, pages 9323–9332. PMLR, 2021.
- [48] Peter W Shor. Algorithms for quantum computation: discrete logarithms and factoring. In *Proceedings 35th annual symposium on foundations of computer science*, pages 124–134. Ieee, 1994.
- [49] Gregory Sliwoski, Sandeepkumar Kothiwale, Jens Meiler, and Edward W Lowe. Computational methods in drug discovery. *Pharmacological reviews*, 66(1):334–395, 2014.
- [50] Jascha Sohl-Dickstein, Eric Weiss, Niru Maheswaranathan, and Surya Ganguli. Deep unsupervised learning using nonequilibrium thermodynamics. In *International conference on machine learning*, pages 2256–2265. PMLR, 2015.
- [51] Jiaming Song, Qinsheng Zhang, Hongxu Yin, Morteza Mardani, Ming-Yu Liu, Jan Kautz, Yongxin Chen, and Arash Vahdat. Loss-guided diffusion models for plug-and-play controllable generation. In *International Conference on Machine Learning*, pages 32483–32498. PMLR, 2023.
- [52] Yang Song, Jascha Sohl-Dickstein, Diederik P Kingma, Abhishek Kumar, Stefano Ermon, and Ben Poole. Score-based generative modeling through stochastic differential equations. *arXiv* preprint arXiv:2011.13456, 2020.
- [53] Jules Tilly, Hongxiang Chen, Shuxiang Cao, Dario Picozzi, Kanav Setia, Ying Li, Edward Grant, Leonard Wossnig, Ivan Rungger, George H Booth, et al. The variational quantum eigensolver: a review of methods and best practices. *Physics Reports*, 986:1–128, 2022.
- [54] Clement Vignac, Igor Krawczuk, Antoine Siraudin, Bohan Wang, Volkan Cevher, and Pascal Frossard. Digress: Discrete denoising diffusion for graph generation. In *The Eleventh International Conference on Learning Representations*, 2023.

- [55] Joseph L Watson, David Juergens, Nathaniel R Bennett, Brian L Trippe, Jason Yim, Helen E Eisenach, Woody Ahern, Andrew J Borst, Robert J Ragotte, Lukas F Milles, et al. De novo design of protein structure and function with rfdiffusion. *Nature*, 620(7976):1089–1100, 2023.
- [56] Lemeng Wu, Chengyue Gong, Xingchao Liu, Mao Ye, and Qiang Liu. Diffusion-based molecule generation with informative prior bridges. Advances in Neural Information Processing Systems, 35:36533–36545, 2022.
- [57] Minkai Xu, Lantao Yu, Yang Song, Chence Shi, Stefano Ermon, and Jian Tang. Geodiff: A geometric diffusion model for molecular conformation generation. arXiv preprint arXiv:2203.02923, 2022.
- [58] Minkai Xu, Alexander S Powers, Ron O Dror, Stefano Ermon, and Jure Leskovec. Geometric latent diffusion models for 3d molecule generation. In *International Conference on Machine Learning*, pages 38592–38610. PMLR, 2023.
- [59] San-Roman, R., Nachmani, E. & Wolf, L. Noise estimation for generative diffusion models. *ArXiv Preprint ArXiv:2104.02600.* (2021)
- [60] Xia, M., Shen, Y., Lei, C., Zhou, Y., Zhao, D., Yi, R., Wang, W. & Liu, Y. Towards More Accurate Diffusion Model Acceleration with A Timestep Tuner. *Proceedings Of The IEEE/CVF Conference On Computer Vision And Pattern Recognition (CVPR)*. pp. 5736-5745 (2024,6)
- [61] Kahouli, K., Hessmann, S., Müller, K., Nakajima, S., Gugler, S. & Gebauer, N. Molecular relaxation by reverse diffusion with time step prediction. *ArXiv Preprint ArXiv:2404.10935*. (2024)
- [62] Ye, Z., Chen, Z., Li, T., Huang, Z., Luo, W. & Qi, G. Schedule On the Fly: Diffusion Time Prediction for Faster and Better Image Generation. *ArXiv Preprint ArXiv:2412.01243*. (2024)
- [63] Cornet, F., Bartosh, G., Schmidt, M. & Naesseth, C. Equivariant neural diffusion for molecule generation. 38th Conference On Neural Information Processing Systems. (2024)

A Method details

A.1 Time Predictor

For model architecture, we use EGNN [47] with L=7 layers, each with hidden dimension $h_f=192$. We use the same split of training / test dataset of QM9.

Time predictor training For completeness, we restate the training of the time predictor (Eq. 10) here. The time predictor is trained for minimizing the cross-entropy loss between the predicted logits $\hat{\mathbf{p}}$ and one-hot vector of the forward timestep t:

$$\mathcal{L}_{\text{time-predictor}}(\boldsymbol{\phi}) = -\mathbb{E}_{t,\mathbf{x}_0} \left[\log \left(\hat{\mathbf{p}}_{\boldsymbol{\phi}}(\mathbf{x}_t)_t \right) \right], \tag{12}$$

where t is uniformly drawn from the interval [0, T].

For conditional diffusion model, we train separate time predictor for each of the target property by concatenating conditional information c to the input \mathbf{x}_t .

The rationale behind using cross-entropy loss rather than simple regression loss is because $p(t|\mathbf{x})$ can not be estimated from the point estimate if there exists intersection between support of marginal distributions p_t and p_s which is from different timesteps s and t, respectively. In other words, this implies there exists $\mathbf{x} \in \mathcal{R}^d$ such that $p_t(\mathbf{x}) > 0$ and $p_s(\mathbf{x}) > 0$ simultaneously holds.

Finally, we train the time predictor within 24 hours with 4 NVIDIA A6000 GPUs.

A.2 Quantum online guidance

Quantum Machine Learning Quantum computing is expected to become a powerful computational tool in the future [14]. While at its early stage, various of quantum machine learning algorithms are proved to have advantage over classical methods [3]. In computational chemistry, these advantages are indeed expected to have huge potential since classically intractable computations like finding ground state for big molecules are expected to become feasible with exponential speed-ups [48] of quantum machines.

Variational Quantum Eigensolver Variational Quantum Eigensolver (VQE) [41] is a near term quantum machine learning algorithm which leverages variational principle to obtain the lowest energy of a molecule with given Hamiltonian. For the given Hamiltonian \hat{H} , trial wave function $|\psi(\theta)\rangle$ which is parameterized by a quantum circuit (θ) is prepared to obtain ground state energy E_0 with following inequality:

$$E_0 \le \frac{\langle \psi(\boldsymbol{\theta}) | \hat{H} | \psi(\boldsymbol{\theta}) \rangle}{\langle \psi(\boldsymbol{\theta}) | \psi(\boldsymbol{\theta}) \rangle}.$$
 (13)

Specifically, parameters θ in quantum circuit is iteratively optimized to minimize the following objective:

$$E(\boldsymbol{\theta}) = \frac{\langle \psi(\boldsymbol{\theta}) | \hat{H} | \psi(\boldsymbol{\theta}) \rangle}{\langle \psi(\boldsymbol{\theta}) | \psi(\boldsymbol{\theta}) \rangle}.$$
 (14)

When quantum circuit θ is expressive enough, one can see that $|\psi(\theta_*)\rangle$, where θ_* is a minimizer of Eq. (14), gives the ground state of the given system. For more comprehensive review with its potential advantages, one may refer to [53].

Quantum online guidance Quantum online guidance is a type of online guidance algorithm where we use VQE-based algorithm to calculate exact values of quantum chemical properties instead of using classifier which is usually a neural network.

In each denoising step of diffusion model, we first apply Tweedie's formula (Eq. 7) to estimate clean molecule $\hat{\mathbf{x}}_0$. Then we use VQE to calculate ground state energy of the estimated molecule by iteratively updating $\boldsymbol{\theta}$ for $E(\hat{\mathbf{x}}_0, \boldsymbol{\theta}) = \langle \psi(\boldsymbol{\theta}) | H(\hat{\mathbf{x}}_0) | \psi(\boldsymbol{\theta}) \rangle$. After obtaining $\boldsymbol{\theta}_{\star}(\hat{\mathbf{x}}_0)$ which minimizes $E(\hat{\mathbf{x}}_0, \boldsymbol{\theta})$, we obtain target property value $E_0(\hat{\mathbf{x}}_0)$. To obtain gradient in Eq. (8), we use zeroth-order method [35] with respect to the position of atoms to obtain gradient as follows:

$$\nabla_{\mathbf{x}_t} \log \mathbb{E}_{\mathbf{x}_0 \sim p(\mathbf{x}_0|\mathbf{x}_t)} p(\mathbf{c}|\hat{\mathbf{x}}_0) \approx -\nabla_{\mathbf{x}_t} E_0(\hat{\mathbf{x}}_0^i) \approx -\sum_{i=1}^k \frac{E_0(\hat{\mathbf{x}}_0^i + \mathbf{h}_i) - E_0(\hat{\mathbf{x}}_0^i - \mathbf{h}_i)}{2\mathbf{h}_i}, \quad (15)$$

where k is a hyperparameter for multipoint estimate when using the zeroth-order optimization.

A.3 Properties of the Zero-Center-of-Mass Subspace

Let $\mathcal{X} = \{\mathbf{x} \in \mathbb{R}^{M \times 3} : \frac{1}{M} \sum_{i=1}^{M} \mathbf{x}_i = \mathbf{0}\}$ be the subspace of $\mathbb{R}^{M \times 3}$ where the center of mass is zero. Here we discuss some properties of \mathcal{X} that are used in the TACS framework. First, note that \mathcal{X} is a linear subspace of $\mathbb{R}^{M \times 3}$ with dimension $(M-1) \times 3$. There exists an isometric isomorphism $\phi: \mathbb{R}^{(M-1) \times 3} \to \mathcal{X}$, i.e., a linear bijective map that preserves distances: $\|\phi(\hat{\mathbf{x}})\| = \|\hat{\mathbf{x}}\|$ for all $\hat{\mathbf{x}} \in \mathbb{R}^{(M-1) \times 3}$. Intuitively, ϕ allows us to map between the lower-dimensional space $\mathbb{R}^{(M-1) \times 3}$ and the constrained subspace \mathcal{X} without distortion. If $\mathbf{x} \in \mathcal{X}$ is a random variable with probability density $q(\mathbf{x})$, then the corresponding density of $\hat{\mathbf{x}} = \phi^{-1}(\mathbf{x})$ in $\mathbb{R}^{(M-1) \times 3}$ is given by $\hat{q}(\hat{\mathbf{x}}) = q(\phi(\hat{\mathbf{x}}))$. Similarly, a conditional density $q(\mathbf{x}|\mathbf{y})$ on \mathcal{X} can be written as $\hat{q}(\hat{\mathbf{x}}|\hat{\mathbf{y}}) = q(\phi(\hat{\mathbf{x}})|\phi(\hat{\mathbf{y}}))$. In practice, computations involving probability densities on \mathcal{X} can be performed in $\mathbb{R}^{(M-1) \times 3}$ and mapped back to \mathcal{X} using ϕ as needed. This allows TACS to efficiently learn and sample from distributions on molecular geometries while preserving translation invariance. For further mathematical details on subspaces defined by center-of-mass constraints, we refer the reader to [29] and [47].

A.4 Classfier-free guidance

For conditional generation, we need conditional score $\nabla_{\mathbf{x}} \log p_t(\mathbf{x}_t | \mathbf{c})$ where \mathbf{c} is our target condition. Classifier-free guidance (CFG) [19] replaces conditional score with combination of unconditional score and conditional score. Here, diffusion model is trained with combination of unlabeled sample $(\mathbf{x}_0, \emptyset)$ and labeled samples $(\mathbf{x}_0, \mathbf{c})$. The reverse diffusion process (Eq. 2) in CFG changes as follows:

$$d\mathbf{x}_{t} = \left[-\frac{1}{2}\beta(t)\mathbf{x}_{t} - \beta(t)\left(-w\nabla_{\mathbf{x}_{t}}\log p_{t}(\mathbf{x}_{t}) + (1+w)\nabla_{\mathbf{x}_{t}}\log p_{t}(\mathbf{x}_{t}|\mathbf{c})\right) \right] dt + \sqrt{\beta(t)} d\bar{\mathbf{w}}_{t}$$
(16)

Here, w is a conditional weight which controls the strength of conditional guidance. When w = -1, the process converges to the unconditional generation and with larger w, one can put more weights on conditional score. In the experiments, we use w = 0 following [23, 5].

B Experimental details

B.1 Synthetic experiment with H_3^+

Here, we provide experimental results on our synthetic experiment. Our results show that TACS is robust through different online guidance strength z and outperforms naive mixture of CFG and OG.

Table 7: MAE with target condition

Table 8: L2 distance from data distribution

Z	CFG+OG	TACS
0	0.4823	0.0817
1	0.0961	0.0530
2	0.1069	0.0438
5	0.1107	0.0377
10	0.1430	0.0529
25	0.5427	0.3089

Z	CFG+OG	TACS
0	0.0386	0.0294
1	0.0653	0.0305
2	0.1886	0.0339
5	0.6553	0.0383
10	3.5112	0.1820
25	18.8983	8.2466

Geometric Optimization It is known that H_3^+ molecule has a ground state energy around -1.34Ha. Assuming we don't have any prior knowledge of this information, we try to generate molecules with conditioning on the target ground state energy -2.0Ha. Applying TACS proves to be strong in this case also, which implies that our method can robustly guide the molecule without destroying distances.

B.2 Experiments on QM9

Dataset details The QM9 dataset [45] is a widely-used benchmark in computational chemistry and machine learning. It contains 134k stable small organic molecules with up to 9 heavy atoms (C, O, N, F) and up to 29 atoms including hydrogen. This size constraint allows the molecules to be exhaustively enumerated and have their quantum properties calculated accurately using density functional theory (DFT). Each molecule in QM9 is specified by its Cartesian coordinates (in Angstroms) of all atoms at equilibrium geometry, along with 12 associated properties calculated from quantum mechanical simulations.

QM9 molecular properties In Table 9, we describe six quantum chemical properties that are used for conditional generation in our experiments.

Property	Description
Polarizability (α)	Measure of a molecule's ability to form instantaneous dipoles in
Totalizability (\alpha)	an external electric field.
HOMO-LUMO gap $(\Delta \epsilon)$	Energy gap between the HOMO and LUMO orbitals, indicating
$110MO-LOMO gap (\Delta \epsilon)$	electronic excitation energies and chemical reactivity.
HOMO energy (ϵ_{HOMO})	Energy of the highest occupied molecular orbital, related to ion-
HOMO energy (e _{HOMO})	ization potential and donor reactivity.
LUMO energy (ϵ_{LUMO})	Energy of the lowest unoccupied molecular orbital, related to
Lowo chergy (eLumo)	electron affinity and acceptor reactivity.
Dipole moment (μ)	Measure of the separation of positive and negative charges in a
Dipote moment (μ)	molecule, indicating polarity.
Heat capacity (C_v)	Measure of how much the temperature of a molecule changes
Theat capacity (\bigcirc_v)	when it absorbs or releases heat.

Table 9: Quantum chemical properties

Performance metrics To evaluate the quality of generated molecules, Table 10 shows descriptions of the metrics that are used in our experiments to check whether generated samples satisfy basic molecular properties.

Property	Description
	Proportion of generated molecules that are chemically valid, as
Validity (Valid)	determined by RDKit. A molecule is valid if RDKit can parse it
	without encountering invalid valences.
Atom Stability (AS)	Percentage of atoms within generated molecules that possess correct valencies. Bond types are predicted based on atom distances and types, and validated against thresholds. An atom is stable if its total bond count matches the expected valency for its atomic number.
Molecule Stability (MS)	Percentage of generated molecules where all constituent atoms are stable.

Table 10: Performance metrics

Baselines We compare our method against Equivariant Diffusion Models (EDM) [23] which learn a rotationally equivariant denoising process for property-conditioned generation and Equivariant Energy Guided SDE (EEGSDE) [5], which guides generation with a learned time-dependent energy function.

Additional baselines Two baselines are employed following the approach outlined by [23]. To measure "Naive (U-Bound)", we disrupt any inherent correlation between molecules and properties by shuffling the property labels in \mathcal{D}_b and evaluating ϕ_c on the modified dataset. "L-Bound" is a lower bound estimation of the predictive capability. This value is obtained by assessing the loss of ϕ_c on \mathcal{D}_b , providing a reference point for the minimum achievable performance. If a proposed model, denoted

as, surpasses the performance of Naive (U-Bound), it indicates successful incorporation of conditional property information into generated molecules. Similarly, outperforming the L-Bound demonstrates the model's capacity to incorporate structural features beyond atom count and capture the intricacies of molecular properties. These baselines establish upper and lower bounds for evaluating mean absolute error (MAE) metrics in conditional generation tasks.

Diffusion model training For a fair comparison with EDM and EEGSDE [23, 5], we adopt their training settings, using model checkpoints provided in the EEGSDE code: https://github.com/gracezhao1997/EEGSDE. The diffusion model is trained for 2000 epochs with a batch size of 64, learning rate of 0.0001, Adam optimizer, and an exponential moving average (EMA) with a decay rate of 0.9999. During evaluation, we generate molecules by first sampling the number of atoms $M \sim p(M)$ and the property value $\mathbf{c} \sim p(\mathbf{c}|M)$. Here p(M) is the distribution of molecule sizes in the training data, and $p(\mathbf{c}|M)$ is the conditional distribution of the property given the molecule size. Then we generate a molecule conditioned on M and \mathbf{c} using the learned reverse process.

Hyperparameters for TACS We analyze different hyperparameter settings for all six quantum chemical properties $(\alpha, \Delta\epsilon, \epsilon_{\text{HOMO}}, \epsilon_{\text{LUMO}}, \mu, C_v)$ for the result in the Table 1. We vary the TCS starting timestep $t_{\text{TCS}} \in \{200, 400, 600, 800\}$, online guidance starting timestep $t_{\text{OG}} \in \{200, 400, 600, 800\}$, online guidance ending timestep $\tilde{t}_{\text{OG}} \in \{10, 20, 30\}$, gradient clipping threshold $\kappa \in \{\infty, 1, 0.1\}$ for Eq. (8), and guidance strength $z \in \{1.5, 1.0, 0.5\}$ in Eq. (9). Except for ϵ_{LUMO} (optimal with z = 0.5, $\tilde{t}_{\text{OG}} = 0$), we find $t_{\text{TCS}} = 600$, $t_{\text{OG}} = 600$, $\tilde{t}_{\text{OG}} = 20$, z = 1, and $\kappa = 1$ consistently achieve low MAE with molecular stability above 80%.

B.3 Additional Experiment Details

B.3.1 Experiments on Geom-Drug

Dataset Details Geom-Drug dataset [4] contains approximately 450K molecules with up to 181 atoms and an average of 44.4 atoms per molecule. Following [5], we split the dataset into training/validation/test sets of 554k/70k/70k samples respectively.

Performance Metrics For each experiment, we generate 10,000 molecular samples for evaluation. As in QM9 experiments, we measure atom stability (AS) and validity (Valid) using RdKit [32].

Time Predictor Training For Geom-Drug, we employ TCS with 4 EGNN layers and 256 hidden features. The time predictor ϕ is trained unconditionally with the same EGNN architecture as QM9 for 10 epochs. During generation, TCS starts from timestep 600 and utilizes a window size of 10 for time correction.

B.3.2 Experiments on Target Structure Generation

Training Details For molecular fingerprint-based structure generation, we follow the evaluation protocol in [5]. The diffusion model architecture remains consistent with our QM9 experiments, using EGNN with 256 hidden features and 4 layers, trained for 10 epochs.

Performance Metrics For evaluation, we use Tanimoto similarity score [16] which measures the structural similarity between generated molecules and target structures through molecular fingerprint comparison. Specifically, let S_g and S_t be the sets of bits that are set to 1 in the fingerprints of generated and target molecules respectively. The Tanimoto similarity is defined as $|S_g \cap S_t|/|S_g \cup S_t|$, where $|\cdot|$ denotes the number of elements in a set. We evaluate the similarity on 10,000 generated samples.

Baselines For both experiments, we directly compare with baseline results reported in [22]. For Geom-Drug unconditional generation, these include ENF [47], G-Schnet [15], GDM variants [57], EDM [23], and EDM-Bridge [56]. For target structure generation, we compare against G-SchNet [15], GDM, GDM-AUG [57], Conditional EDM [23], and EEGSDE [5] with various guidance scales.

C Additional experiments

C.1 When to apply TCS and OG

We ablate when to start the time-corrected sampling (TCS) and online guidance (OG) during the reverse diffusion process. The notation $t_{\rm TCS}$ and $t_{\rm OG}$ indicates we apply TCS after timestep $t_{\rm TCS}$ and OG after the timestep $t_{\rm OG}$ in the reverse diffusion process. We report results for property $\epsilon_{\rm LUMO}$ in Table 11. The result shows that applying TACS from early steps (t=600,800) generates samples best satisfying the target condition but with less molecular stability and validity. In contrast, when we start applying TACS after later step t=400, generated samples have higher MAE, MS, and Validity. Interstingly, if we apply TACS only in the later part (after t=200), MAE, MS, and validity decreases again. We leave further investigation on this phenomenon and explanation for future works.

In our experiments, we use $t_{TCS} = t_{OG} = 600$ as our default setting.

Table 11: Ablation study on when to start time-corrected sampling (TCS) and online guidance (OG) during the reverse diffusion process for the target property ϵ_{LUMO} . We use z=1 for the experiment. The best value in each column is bolded.

$[t_{TCS}, t_{OG}]$	MAE	MS (%)	Valid (%)
[800, 800]	236	74.9	86.3
[600, 600]	236	74.9	86.2
[400, 400]	360	86.6	93.3
[200, 200]	248	72.1	84.5

C.2 Number of MC samples

Additional experiments are conducted on the effect of number of MC samples m in Eq. (8). LGD [51] estimates \mathbf{x}_0 assuming $q(\mathbf{x}_0|\mathbf{x}_t)$ is a normal distribution with mean $\hat{\mathbf{x}}_0$ (Eq. 7) and variance σ^2 which is a hyperparameter.

First, we investigate the effect of varying the variance σ in MC sampling. Table 12 shows that the result is robust in the small values of σ but when σ is larger than some point, quality of generated samples decreases (higher MAE and lower MS).

Next, we test how the performance of TACS is affected by number of MC samples m. Table 13 shows that performance of TACS is robust in number of MC samples but we did not observe any performance increase with the number of MC samples as in [18].

Table 12: MC effect with varying σ . 5 MC samples are used and the target property is α .

σ	MAE	MS (%)
0.0001	1.506	86.06
0.0005	1.390	84.33
0.001	1.501	86.92
0.005	1.395	86.35
0.01	1.464	85.10
0.05	1.801	85.04
0.1	2.186	82.69
0.3	2.936	75.67

Table 13: Varying number of MC samples with $\sigma = 0.005$. Target property is α .

# Samples	MAE	MS (%)
1	1.440	86.10
5	1.395	86.35
10	1.505	82.21
15	1.545	83.04
20	1.468	86.76

C.3 Results on Novelty, Uniqueness

We report additional metrics on the novelty, uniqueness of generated molecules in Table 14 following previous literature [5, 23, 58]. Novelty measures the percentage of generated molecules not seen in the training set. Uniqueness measures the proportion of non-isomorphic graphs within valid molecules. Higher values indicate better quality for both metrics. The result shows that TACS generates molecules with decreased novelty. This shows that TACS is effective in making generated molecules that stick to the original data distribution while satisfying to meet the target condition.

Table 14: Novelty and uniqueness of generated sample for the target property ϵ_{LUMO} .

Method	Novelty (%)	Uniqueness (%)	
EDM	84.5	99.9	
EEGSDE	84.8	84.8	
TACS	71.6	99.8	

D Mathematical Derivations

In our derivation of equivariance properties of the time predictor, we closely adhere to the formal procedures outlined in [23, 57, 47].

Definition 1 (E(3) Equivariance). A function $f: \mathbb{R}^{N \times 3} \to \mathbb{R}^{N \times d}$ is E(3)-equivariant if for any orthogonal matrix $\mathbf{R} \in \mathbb{R}^{3 \times 3}$ and translation vector $\mathbf{v} \in \mathbb{R}^3$,

$$f(\mathbf{RX} + \mathbf{v1}^{\top}) = \mathbf{R} \cdot f(\mathbf{X}), \tag{17}$$

where $\mathbf{X} \in \mathbb{R}^{N \times 3}$ and $\mathbf{1} \in \mathbb{R}^N$ is the all-ones vector.

Definition 2 (Permutation Invariance). A function $g: \mathbb{R}^{N \times d} \to \mathbb{R}^d$ is permutation-invariant if for any permutation matrix $\mathbf{P} \in \{0,1\}^{N \times N}$,

$$g(\mathbf{PH}) = g(\mathbf{H}),\tag{18}$$

where $\mathbf{H} \in \mathbb{R}^{N \times d}$.

Proposition 1. Let $f: \mathbb{R}^{N \times 3} \to \mathbb{R}^{N \times d}$ be an E(3)-equivariant function and $g: \mathbb{R}^{N \times d} \to \mathbb{R}^d$ be a permutation-invariant function. Then, the composition $h = g \circ f: \mathbb{R}^{N \times 3} \to \mathbb{R}^d$ is invariant to E(3) transformations, i.e.,

$$h(\mathbf{RX} + \mathbf{v1}^{\top}) = h(\mathbf{X}). \tag{19}$$

Proof. For any orthogonal matrix $\mathbf{R} \in \mathbb{R}^{3 \times 3}$ and translation vector $\mathbf{v} \in \mathbb{R}^3$,

$$h(\mathbf{R}\mathbf{X} + \mathbf{v}\mathbf{1}^{\top}) = g(f(\mathbf{R}\mathbf{X} + \mathbf{v}\mathbf{1}^{\top}))$$

$$= g(\mathbf{R} \cdot f(\mathbf{X})) \quad (E(3) \text{ equivariance of } f)$$

$$= g(f(\mathbf{X})) \quad (Permutation invariance of g)$$

$$= h(\mathbf{X}). \tag{20}$$

Theorem 1 (Time Predictor Equivariance). Let $\mathcal{G} = (\mathcal{V}, \mathcal{E})$ be a graph representing a molecule, where $\mathcal{V} = \{1, \dots, N\}$ is the set of nodes (atoms) and $\mathcal{E} \subseteq \mathcal{V} \times \mathcal{V}$ is the set of edges (bonds). Let $\mathbf{X}_t \in \mathbb{R}^{N \times 3}$ denote the atomic coordinates and $\mathbf{c} \in \mathbb{R}^d$ be a condition vector at diffusion timestep t. Consider a time predictor $p_{\phi}(t|\mathbf{X}_t,\mathbf{c}) = \operatorname{softmax}(f_{\phi}(\mathbf{X}_t,\mathbf{c}))$ parameterized by a composition of an E(3)-equivariant graph neural network $EGNN_{\phi} : \mathbb{R}^{N \times 3} \times \mathbb{R}^{N \times d_h} \times \mathbb{R}^d \to \mathbb{R}^{N \times d'}$, a permutation-invariant readout function $\rho : \mathbb{R}^{N \times d'} \to \mathbb{R}^{d'}$, and a multilayer perceptron $\psi : \mathbb{R}^{d'} \to \mathbb{R}^T$, i.e.,

$$f_{\phi}(\mathbf{X}_{t}, \mathbf{c}) = \psi(\rho(EGNN_{\phi}(\mathbf{X}_{t}, \mathbf{H}_{t}, \mathbf{c}))), \tag{21}$$

where $\mathbf{H}_t \in \mathbb{R}^{N \times d_h}$ are node features and T is the total number of diffusion timesteps. Then, the time predictor $p_{\phi}(t|\mathbf{X}_t, \mathbf{c})$ is invariant to E(3) transformations, i.e., for any orthogonal matrix $\mathbf{R} \in \mathbb{R}^{3 \times 3}$ and translation vector $\mathbf{v} \in \mathbb{R}^3$,

$$p_{\phi}(t|\mathbf{R}\mathbf{X}_t + \mathbf{v}\mathbf{1}^{\top}, \mathbf{c}) = p_{\phi}(t|\mathbf{X}_t, \mathbf{c}), \quad \forall t \in \{1, \dots, T\}.$$
(22)

Proof. The E(3)-equivariant graph neural network EGNN $_{\phi}$ satisfies [47]:

$$EGNN_{\phi}(\mathbf{R}\mathbf{X}_{t} + \mathbf{v}\mathbf{1}^{\top}, \mathbf{H}_{t}, \mathbf{c}) = \mathbf{R} \cdot EGNN_{\phi}(\mathbf{X}_{t}, \mathbf{H}_{t}, \mathbf{c}). \tag{23}$$

By the permutation invariance of ρ and the invariance of ψ to orthogonal transformations, we have:

$$f_{\phi}(\mathbf{R}\mathbf{X}_{t} + \mathbf{v}\mathbf{1}^{\top}, \mathbf{c}) = \psi(\rho(\mathsf{EGNN}_{\phi}(\mathbf{R}\mathbf{X}_{t} + \mathbf{v}\mathbf{1}^{\top}, \mathbf{H}_{t}, \mathbf{c})))$$

$$= \psi(\rho(\mathbf{R} \cdot \mathsf{EGNN}_{\phi}(\mathbf{X}_{t}, \mathbf{H}_{t}, \mathbf{c})))$$

$$= \psi(\rho(\mathsf{EGNN}_{\phi}(\mathbf{X}_{t}, \mathbf{H}_{t}, \mathbf{c})))$$

$$= f_{\phi}(\mathbf{X}_{t}, \mathbf{c}). \tag{24}$$

Consequently,

$$p_{\phi}(t|\mathbf{R}\mathbf{X}_{t} + \mathbf{v}\mathbf{1}^{\top}, \mathbf{c}) = \operatorname{softmax}(f_{\phi}(\mathbf{R}\mathbf{X}_{t} + \mathbf{v}\mathbf{1}^{\top}, \mathbf{c}))$$
$$= \operatorname{softmax}(f_{\phi}(\mathbf{X}_{t}, \mathbf{c}))$$
$$= p_{\phi}(t|\mathbf{X}_{t}, \mathbf{c}). \tag{25}$$

E Comparison with other related works

While with different motivations and methods, here, we list some of the relevant works and compare their algorithms with ours.

Comparison with DMCMC DMCMC [28] trains a classifier to predict noise levels of the given data during the reverse diffusion process which is similar to our time predictor. However, they use the classifier to estimate the current noise state when conducting MCMC on the product space of the data and the noise. In contrast, our time predictor directly predicts timesteps for correction in diffusion sampling itself. Moreover, while the purpose of noise prediction in DMCMC is for fast sampling, our work use time predictor to accurately produce samples from the desired data distribution.

Comparison with TS-DPM Time-Shift Sampler [34] targets to reduce exposure bias targets similar approach of fixing timesteps during the inference as our time correction method. However, while our method directly selects timesteps based on the time predictor, which has demonstrated robustness in our experiments [34] selects timesteps by calculating variance of image pixels at each step and matching the noise level from the predefined noise schedule which is often inaccurate and expensive. Moreover corrected timestep in [34] is used directly for the start of the next step, while our approach maintains the predefined timestep after accurately estimate clean sample by corrected time step (line 9 in Algorithm 1). By taking every single diffusion step while carefully using predicted time, TACS / TCS can generate samples closer to the target distribution.

To further validate our approach, we provide additional experimental results comparing TS-DDPM [34] and TACS on the QM9 dataset with step size 10. The result in Table 15 shows consistent improvements across various quantum properties which shows the robustness of our approach.

Table 15: Comparison between TACS and Time shift sampler on conditional molecular generation.

	TS-DDPM		TACS (ours)	
Method	MAE	MS (%)	MAE	MS (%)
$\overline{C_v}$	1.066	74.89	0.659	83.6
μ	1.166	73.55	0.387	83.3
α	2.777	75.20	1.44	86.0
$\Delta(\epsilon)$	665.3	82.72	332	88.8
HOMO	371.8	72.74	168	87.3
LUMO	607.6	74.98	289	82.7

F Visualization of generated molecules

Conditional generation with target quantum chemical property

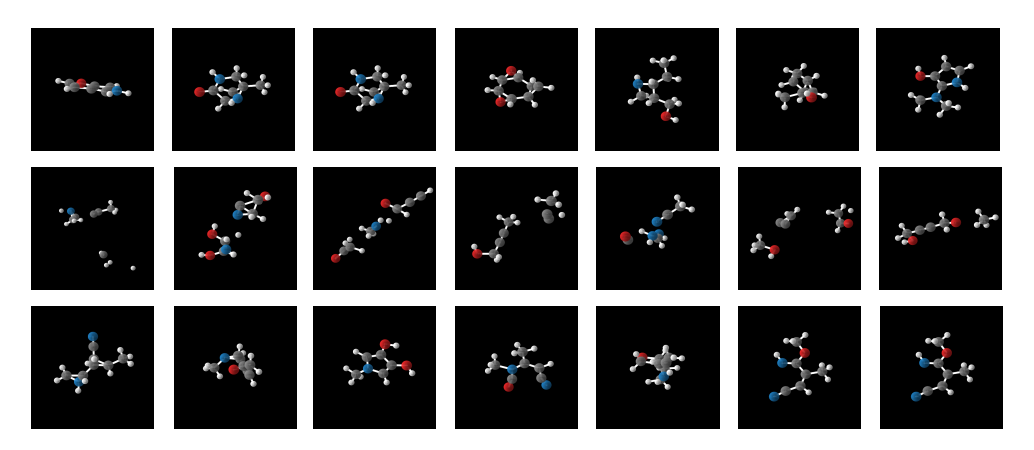


Figure 4: Conditional generation of target property α on QM9. Visualization of molecules generated by TCS (top), online guidance (middle), and TACS (bottom).

Conditional generation with target structure

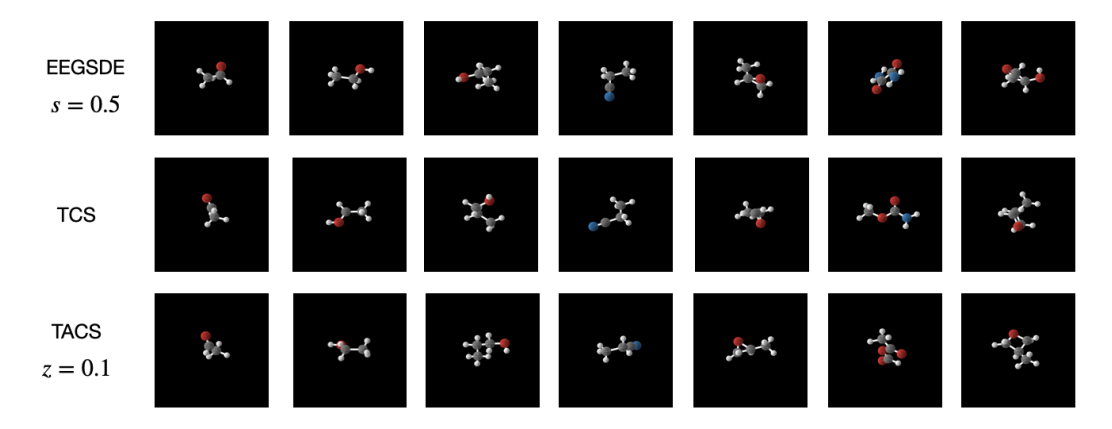


Figure 5: Visualization of how generated molecules align with target structures.

Unconditional generation on Geom-Drug

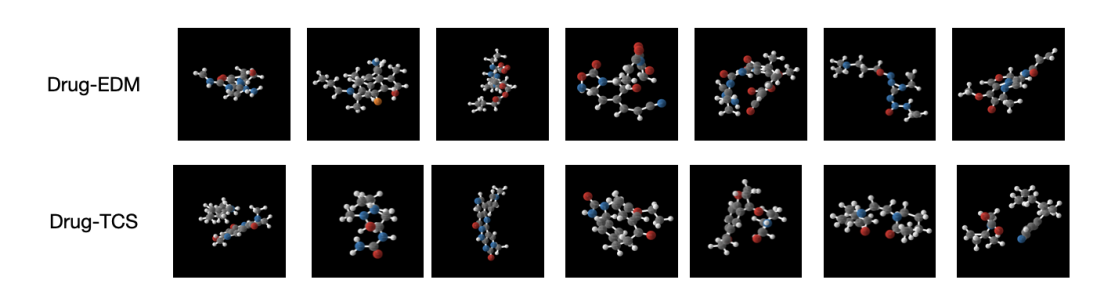


Figure 6: Selection of samples generated by the denoising process of EDM and TCS in Geom-Drug.

NeurIPS Paper Checklist

1. Claims

Question: Do the main claims made in the abstract and introduction accurately reflect the paper's contributions and scope?

Answer: [Yes]

Justification: In the experiments with QM9 datset, we demonstrate our algorithm has superior performance compared to other baselines.

Guidelines:

- The answer NA means that the abstract and introduction do not include the claims made in the paper.
- The abstract and/or introduction should clearly state the claims made, including the contributions made in the paper and important assumptions and limitations. A No or NA answer to this question will not be perceived well by the reviewers.
- The claims made should match theoretical and experimental results, and reflect how much the results can be expected to generalize to other settings.
- It is fine to include aspirational goals as motivation as long as it is clear that these goals are not attained by the paper.

2. Limitations

Question: Does the paper discuss the limitations of the work performed by the authors?

Answer: [Yes]

Justification: We put limitations of our work in Section 7.

Guidelines:

- The answer NA means that the paper has no limitation while the answer No means that the paper has limitations, but those are not discussed in the paper.
- The authors are encouraged to create a separate "Limitations" section in their paper.
- The paper should point out any strong assumptions and how robust the results are to violations of these assumptions (e.g., independence assumptions, noiseless settings, model well-specification, asymptotic approximations only holding locally). The authors should reflect on how these assumptions might be violated in practice and what the implications would be.
- The authors should reflect on the scope of the claims made, e.g., if the approach was only tested on a few datasets or with a few runs. In general, empirical results often depend on implicit assumptions, which should be articulated.
- The authors should reflect on the factors that influence the performance of the approach. For example, a facial recognition algorithm may perform poorly when image resolution is low or images are taken in low lighting. Or a speech-to-text system might not be used reliably to provide closed captions for online lectures because it fails to handle technical jargon.
- The authors should discuss the computational efficiency of the proposed algorithms and how they scale with dataset size.
- If applicable, the authors should discuss possible limitations of their approach to address problems of privacy and fairness.
- While the authors might fear that complete honesty about limitations might be used by reviewers as grounds for rejection, a worse outcome might be that reviewers discover limitations that aren't acknowledged in the paper. The authors should use their best judgment and recognize that individual actions in favor of transparency play an important role in developing norms that preserve the integrity of the community. Reviewers will be specifically instructed to not penalize honesty concerning limitations.

3. Theory Assumptions and Proofs

Question: For each theoretical result, does the paper provide the full set of assumptions and a complete (and correct) proof?

75936

Answer: [NA]

Justification: The paper does not include theoretical results.

Guidelines:

- The answer NA means that the paper does not include theoretical results.
- All the theorems, formulas, and proofs in the paper should be numbered and cross-referenced.
- All assumptions should be clearly stated or referenced in the statement of any theorems.
- The proofs can either appear in the main paper or the supplemental material, but if they appear in the supplemental material, the authors are encouraged to provide a short proof sketch to provide intuition.
- Inversely, any informal proof provided in the core of the paper should be complemented by formal proofs provided in appendix or supplemental material.
- Theorems and Lemmas that the proof relies upon should be properly referenced.

4. Experimental Result Reproducibility

Question: Does the paper fully disclose all the information needed to reproduce the main experimental results of the paper to the extent that it affects the main claims and/or conclusions of the paper (regardless of whether the code and data are provided or not)?

Answer: [Yes]

Justification: In Appendix B, we provide experimental details for all of our experiments.

Guidelines:

- The answer NA means that the paper does not include experiments.
- If the paper includes experiments, a No answer to this question will not be perceived well by the reviewers: Making the paper reproducible is important, regardless of whether the code and data are provided or not.
- If the contribution is a dataset and/or model, the authors should describe the steps taken to make their results reproducible or verifiable.
- Depending on the contribution, reproducibility can be accomplished in various ways. For example, if the contribution is a novel architecture, describing the architecture fully might suffice, or if the contribution is a specific model and empirical evaluation, it may be necessary to either make it possible for others to replicate the model with the same dataset, or provide access to the model. In general, releasing code and data is often one good way to accomplish this, but reproducibility can also be provided via detailed instructions for how to replicate the results, access to a hosted model (e.g., in the case of a large language model), releasing of a model checkpoint, or other means that are appropriate to the research performed.
- While NeurIPS does not require releasing code, the conference does require all submissions to provide some reasonable avenue for reproducibility, which may depend on the nature of the contribution. For example
- (a) If the contribution is primarily a new algorithm, the paper should make it clear how to reproduce that algorithm.
- (b) If the contribution is primarily a new model architecture, the paper should describe the architecture clearly and fully.
- (c) If the contribution is a new model (e.g., a large language model), then there should either be a way to access this model for reproducing the results or a way to reproduce the model (e.g., with an open-source dataset or instructions for how to construct the dataset).
- (d) We recognize that reproducibility may be tricky in some cases, in which case authors are welcome to describe the particular way they provide for reproducibility. In the case of closed-source models, it may be that access to the model is limited in some way (e.g., to registered users), but it should be possible for other researchers to have some path to reproducing or verifying the results.

5. Open access to data and code

Question: Does the paper provide open access to the data and code, with sufficient instructions to faithfully reproduce the main experimental results, as described in supplemental material?

Answer: [No]

Justification: We provide experimental details and will provide code after it is polished.

Guidelines:

- The answer NA means that paper does not include experiments requiring code.
- Please see the NeurIPS code and data submission guidelines (https://nips.cc/public/guides/CodeSubmissionPolicy) for more details.
- While we encourage the release of code and data, we understand that this might not be possible, so "No" is an acceptable answer. Papers cannot be rejected simply for not including code, unless this is central to the contribution (e.g., for a new open-source benchmark).
- The instructions should contain the exact command and environment needed to run to reproduce the results. See the NeurIPS code and data submission guidelines (https://nips.cc/public/guides/CodeSubmissionPolicy) for more details.
- The authors should provide instructions on data access and preparation, including how to access the raw data, preprocessed data, intermediate data, and generated data, etc.
- The authors should provide scripts to reproduce all experimental results for the new proposed method and baselines. If only a subset of experiments are reproducible, they should state which ones are omitted from the script and why.
- At submission time, to preserve anonymity, the authors should release anonymized versions (if applicable).
- Providing as much information as possible in supplemental material (appended to the paper) is recommended, but including URLs to data and code is permitted.

6. Experimental Setting/Details

Question: Does the paper specify all the training and test details (e.g., data splits, hyper-parameters, how they were chosen, type of optimizer, etc.) necessary to understand the results?

Answer: [Yes]

Justification: In Section 5 and Appendix B, we provide details of our experiments.

Guidelines:

- The answer NA means that the paper does not include experiments.
- The experimental setting should be presented in the core of the paper to a level of detail that is necessary to appreciate the results and make sense of them.
- The full details can be provided either with the code, in appendix, or as supplemental material.

7. Experiment Statistical Significance

Question: Does the paper report error bars suitably and correctly defined or other appropriate information about the statistical significance of the experiments?

Answer: [Yes]

Justification: We verified our algorithm with enough number of iterations and with different types of chemical properties.

Guidelines:

- The answer NA means that the paper does not include experiments.
- The authors should answer "Yes" if the results are accompanied by error bars, confidence intervals, or statistical significance tests, at least for the experiments that support the main claims of the paper.
- The factors of variability that the error bars are capturing should be clearly stated (for example, train/test split, initialization, random drawing of some parameter, or overall run with given experimental conditions).
- The method for calculating the error bars should be explained (closed form formula, call to a library function, bootstrap, etc.)
- The assumptions made should be given (e.g., Normally distributed errors).

- It should be clear whether the error bar is the standard deviation or the standard error
 of the mean.
- It is OK to report 1-sigma error bars, but one should state it. The authors should preferably report a 2-sigma error bar than state that they have a 96% CI, if the hypothesis of Normality of errors is not verified.
- For asymmetric distributions, the authors should be careful not to show in tables or figures symmetric error bars that would yield results that are out of range (e.g. negative error rates).
- If error bars are reported in tables or plots, The authors should explain in the text how they were calculated and reference the corresponding figures or tables in the text.

8. Experiments Compute Resources

Question: For each experiment, does the paper provide sufficient information on the computer resources (type of compute workers, memory, time of execution) needed to reproduce the experiments?

Answer: [Yes]

Justification: We describe the computer resources used in the Appendix $\bf A$ and relevant references for the model checkpoints in Appendix $\bf B$.

Guidelines:

- The answer NA means that the paper does not include experiments.
- The paper should indicate the type of compute workers CPU or GPU, internal cluster, or cloud provider, including relevant memory and storage.
- The paper should provide the amount of compute required for each of the individual experimental runs as well as estimate the total compute.
- The paper should disclose whether the full research project required more compute than the experiments reported in the paper (e.g., preliminary or failed experiments that didn't make it into the paper).

9. Code Of Ethics

Question: Does the research conducted in the paper conform, in every respect, with the NeurIPS Code of Ethics https://neurips.cc/public/EthicsGuidelines?

Answer: [Yes]

Justification: We follow Code of Ethics during the research.

Guidelines:

- The answer NA means that the authors have not reviewed the NeurIPS Code of Ethics.
- If the authors answer No, they should explain the special circumstances that require a
 deviation from the Code of Ethics.
- The authors should make sure to preserve anonymity (e.g., if there is a special consideration due to laws or regulations in their jurisdiction).

10. Broader Impacts

Question: Does the paper discuss both potential positive societal impacts and negative societal impacts of the work performed?

Answer: [Yes]

Justification: We include a Societal Impact statement in Section 7. We note that de novo molecular generation can be of great importance for the discovery of new drug compounds as well as new materials. Naturally, there is a small risk of potentially malicious or unintended use (i.e. generating harmful compounds).

Guidelines:

- The answer NA means that there is no societal impact of the work performed.
- If the authors answer NA or No, they should explain why their work has no societal impact or why the paper does not address societal impact.

- Examples of negative societal impacts include potential malicious or unintended uses (e.g., disinformation, generating fake profiles, surveillance), fairness considerations (e.g., deployment of technologies that could make decisions that unfairly impact specific groups), privacy considerations, and security considerations.
- The conference expects that many papers will be foundational research and not tied to particular applications, let alone deployments. However, if there is a direct path to any negative applications, the authors should point it out. For example, it is legitimate to point out that an improvement in the quality of generative models could be used to generate deepfakes for disinformation. On the other hand, it is not needed to point out that a generic algorithm for optimizing neural networks could enable people to train models that generate Deepfakes faster.
- The authors should consider possible harms that could arise when the technology is being used as intended and functioning correctly, harms that could arise when the technology is being used as intended but gives incorrect results, and harms following from (intentional or unintentional) misuse of the technology.
- If there are negative societal impacts, the authors could also discuss possible mitigation strategies (e.g., gated release of models, providing defenses in addition to attacks, mechanisms for monitoring misuse, mechanisms to monitor how a system learns from feedback over time, improving the efficiency and accessibility of ML).

11. Safeguards

Question: Does the paper describe safeguards that have been put in place for responsible release of data or models that have a high risk for misuse (e.g., pretrained language models, image generators, or scraped datasets)?

Answer: [NA]

Justification: Molecular generation has less risk for misuse.

Guidelines:

- The answer NA means that the paper poses no such risks.
- Released models that have a high risk for misuse or dual-use should be released with
 necessary safeguards to allow for controlled use of the model, for example by requiring
 that users adhere to usage guidelines or restrictions to access the model or implementing
 safety filters.
- Datasets that have been scraped from the Internet could pose safety risks. The authors should describe how they avoided releasing unsafe images.
- We recognize that providing effective safeguards is challenging, and many papers do
 not require this, but we encourage authors to take this into account and make a best
 faith effort.

12. Licenses for existing assets

Question: Are the creators or original owners of assets (e.g., code, data, models), used in the paper, properly credited and are the license and terms of use explicitly mentioned and properly respected?

Answer: [Yes]

Justification: We properly credit the original owners of assets used in the paper.

Guidelines:

- The answer NA means that the paper does not use existing assets.
- The authors should cite the original paper that produced the code package or dataset.
- The authors should state which version of the asset is used and, if possible, include a URL.
- The name of the license (e.g., CC-BY 4.0) should be included for each asset.
- For scraped data from a particular source (e.g., website), the copyright and terms of service of that source should be provided.
- If assets are released, the license, copyright information, and terms of use in the
 package should be provided. For popular datasets, paperswithcode.com/datasets
 has curated licenses for some datasets. Their licensing guide can help determine the
 license of a dataset.

- For existing datasets that are re-packaged, both the original license and the license of the derived asset (if it has changed) should be provided.
- If this information is not available online, the authors are encouraged to reach out to the asset's creators.

13. New Assets

Question: Are new assets introduced in the paper well documented and is the documentation provided alongside the assets?

Answer: [NA]

Justification: We do not release new assets.

Guidelines:

- The answer NA means that the paper does not release new assets.
- Researchers should communicate the details of the dataset/code/model as part of their submissions via structured templates. This includes details about training, license, limitations, etc.
- The paper should discuss whether and how consent was obtained from people whose asset is used.
- At submission time, remember to anonymize your assets (if applicable). You can either create an anonymized URL or include an anonymized zip file.

14. Crowdsourcing and Research with Human Subjects

Question: For crowdsourcing experiments and research with human subjects, does the paper include the full text of instructions given to participants and screenshots, if applicable, as well as details about compensation (if any)?

Answer: [NA]

Justification: Our work does not involve crowdsourcing nor research with human subjects. Guidelines:

- The answer NA means that the paper does not involve crowdsourcing nor research with human subjects.
- Including this information in the supplemental material is fine, but if the main contribution of the paper involves human subjects, then as much detail as possible should be included in the main paper.
- According to the NeurIPS Code of Ethics, workers involved in data collection, curation, or other labor should be paid at least the minimum wage in the country of the data collector.

15. Institutional Review Board (IRB) Approvals or Equivalent for Research with Human Subjects

Question: Does the paper describe potential risks incurred by study participants, whether such risks were disclosed to the subjects, and whether Institutional Review Board (IRB) approvals (or an equivalent approval/review based on the requirements of your country or institution) were obtained?

Answer: [NA]

Justification: Our work does not involve crowdsourcing nor research with human subjects. Guidelines:

- The answer NA means that the paper does not involve crowdsourcing nor research with human subjects.
- Depending on the country in which research is conducted, IRB approval (or equivalent) may be required for any human subjects research. If you obtained IRB approval, you should clearly state this in the paper.
- We recognize that the procedures for this may vary significantly between institutions and locations, and we expect authors to adhere to the NeurIPS Code of Ethics and the guidelines for their institution.
- For initial submissions, do not include any information that would break anonymity (if applicable), such as the institution conducting the review.